

Estimation of dibaryon $(\Omega^-\Omega^-)_{J\pi=0^+}$ yields at RHIC energies

Zhong-Dao Lu

*China Institute of Atomic Energy, P. O. Box 275(18), Beijing 102413, China, and
China Center of Advance Science and Technology (CCAST), Beijing 100080,
China*

Abstract

The yields of dibaryon $(\Omega\Omega)_{0^+}$ in relativistic heavy ion collisions at three energies (AGS, SPS and RHIC energies) are calculated in the framework of statistical model. It's yield at full RHIC energy, $\sqrt{s_{NN}} = 200$ GeV, is predicted by means of extrapolation. In the RHIC energy region (RHIC to full RHIC energies), it is in order of magnitude $10^{-4} - 10^{-3}$. The yields of hyperon Ω^- and the ratios of $(\Omega\Omega)_{0^+}$ to Ω^- are also given. In the RHIC energy region, the yield of Ω^- is in order of $10^0 - 10^1$ and the ratio of $(\Omega\Omega)_{0^+}$ to Ω^- is $\simeq 1.0 \times 10^{-4}$.

Key words: Dibaryon yield, RHIC energy, Thermal production
PACS: 14.20.Pt, 25.75.-q, 25.75.Dw

1 Introduction

According to quantum chromodynamics (QCD) theory, there is the possibility of the existence of some exotic multi-quark states, such as H dibaryon [1], and gluonic states. The growing interest of searching for such states lies on not only to examine the quantum chromodynamics (QCD) theory, but also to reveal the quark-gluon behavior in short distance and other new physical characteristics. But so far no convinced evidence is found in experiments to show their existence. Recently a new candidate, the strange dibaryon $(\Omega\Omega)_{0^+}$, is suggested and studied based on the chiral SU(3) quark model [2-6]. This six-quark states with large strangeness is found to have more attractive characteristics than other six-quark states. First, it is a deeply bound state. Although the color magnetic interaction in the one gluon exchange term for this diomega system exhibits the repulsive feature, the large attraction stemming from the chiral gluon coupling and from the symmetry property of the system lead to a considerable binding. By the Resonating Group Method, the

binding energy of $(\Omega\Omega)_{0+}$ is found to be as large as ≈ 116 MeV, and the root-mean-square distance between two Ω^- s is 0.84 fm. Second, $(\Omega\Omega)_{0+}$ has a quite long lifetime of $\sim 10^{-10}$ sec as it can undergo only weak decay, such as $(\Omega\Omega)_{0+} \rightarrow \pi^- + \Xi^0 + \Omega^-$ and $(\Omega\Omega)_{0+} \rightarrow \pi^0 + \Xi^- + \Omega^-$. As they are three-body decay, the final state phase-space would be suppressed. In the sudden approximation, the lifetime of $(\Omega\Omega)_{0+}$ was found to be four times longer than the free Ω^- lifetime of 0.822×10^{-10} sec. Apart from these conventional decay modes, the non-meson decay $(\Omega\Omega)_{0+} \rightarrow \Xi^0 + \Omega^-$ is also possible, the lifetime of $(\Omega\Omega)_{0+}$ for this process is twice the free Ω^- lifetime. Third, $(\Omega\Omega)_{0+}$ has two negative charges. These properties make it easily be identified in experiment when it were created.

Because of the large strangeness and very heavy mass, $(\Omega\Omega)_{0+}$ is not likely to be produced in proton-proton collisions. While in relativistic heavy ion collisions, it is found that the strangeness production is enhanced and has been suggested as one of the possible signals of quark-gluon-plasma (QGP). Recent experiments by the WA97 Collaboration [7] and the NA49 Collaboration [8] showed the substantial enhancement of the (anti-)hyperon (Λ , Ξ and Ω) yields in 158 A GeV/c Pb+Pb central collisions relative to p+Pb collisions, and exhibited the enhancement pattern increasing with the strangeness content of the (anti-)hyperon. Therefore, the extreme environment of very hot and very dense block of matter provided by the relativistic heavy ion collisions may lead to the formation of exotic deeply bound objects composed of quarks or baryons with large strangeness, among them the dibaryon $(\Omega\Omega)_{0+}$ is the most possible candidate.

Theoretically, the yields of $(\Omega\Omega)_{0+}$ can be estimated by two ways: The kinetic simulation or microscopic transportation model, and the quantum statistical model or thermal model. Because the formation probability of $(\Omega\Omega)_{0+}$ is very low and the cross sections related to $(\Omega\Omega)_{0+}$ formations and decays are not well known, the calculations by kinetic simulation can not be well carried out. Contrarily, the statistical model can do the calculations easier. Based on this model, ref. 5 gave out an estimation of $(\Omega\Omega)_{0+}$ yields in Pb+Pb collisions at 158A GeV/c (SPS), which is in order of magnitude 10^{-5} . In this paper, we will present its yields in other two reactions: Au+Au collision at 11.6A GeV/c (AGS) and Au+Au collision at $\sqrt{s_{NN}} = 130$ GeV (RHIC). And, based on the results of these three reactions, we try to predict the yield of $(\Omega\Omega)_{0+}$ for Au+Au collision at full RHIC energy, $\sqrt{s_{NN}} = 200$ GeV, by means of extrapolation. In order to reduce the effect of system size to the extrapolated results, the above collisions are chosen to have the same or similar reaction system. The yields of Ω^- and the ratios of $(\Omega\Omega)_{0+}$ to Ω^- are also given.

2 Thermal Production

In relativistic heavy ion collisions, a large amount of particles including baryons, mesons, their resonance and anti-particles are produced and form a fireball of hadronic gases with high particle density and high energy density. The fireball undergoes the expansion until freeze out. The large amount of produced particles and the violent collisions between them lead the gaseous particles inside the fireball to reach the chemical and thermal equilibrium. Such gas system can be described by the statistical model or thermal model. This model has been successfully applied in analysis of hadron yields and ratios at AGS and SPS energies [9–18], and recently the RHIC energy [19,20]. Here we use this model to estimate the yields of $(\Omega\Omega)_{0+}$ in above three energies and predict its yield in full RHIC energy, $\sqrt{s_{NN}} = 200$ GeV, by means of extrapolation.

In the frame of grand canonical ensemble, the density of hadron species i reads as (in unit of $c = \hbar = k_B = 1$)

$$\rho_i = \frac{g_i}{(2\pi)^3} \int_0^\infty \frac{d^3q}{e^{(\varepsilon - \mu_i)/T} \pm 1}, \quad (1)$$

where T is the temperature of the fireball, $\varepsilon = \sqrt{q^2 + m_i^2}$ is the energy of the particle, q and m_i are the momentum and mass, g_i is the spin-isospin degeneracy. \pm stands for the characteristics of statistics, $+$ is for the Fermions and $-$ is for the Bosons. The chemical potential is determined by $\mu_i = B_i\mu_B + S_i\mu_S$, μ_B and μ_S are the chemical potentials of baryon and strangeness respectively, B_i and S_i are the baryon charges and strangeness charges of the particle respectively.

Since the temperature of the fireball is very high, it is reasonable to treat the hadron gas as the ideal gas obeying the Boltzmann distribution. In the condition of $m/T \gg 1$, the density of species i can be well approximated by

$$\rho_i = g_i \left(\frac{m_i T}{2\pi}\right)^{3/2} e^{-(m_i - \mu_i)/T}. \quad (2)$$

We carried out the calculations for the following three relativistic heavy ion collisions: Au+Au collision at 11.6A GeV/ c (AGS), Pb+Pb collision at 158A GeV/ c (SPS) and Au+Au collision at $\sqrt{s_{NN}} = 130$ GeV (RHIC). The experimental data of the hadron yields and ratios are adopted from [10,12,19] and the references therein, respectively. All hadrons including baryons, mesons and possible anti-particles with mass less than 2 GeV/ c^2 are included in the hadron gas of the fireball. The calculations are carried out within the frame of two-source statistical model (TSM) [17,18,20]. This model is developed on

the basis of the standard statistical model, the single-source model (SM), and takes the non-homogeneous effect of the source into account. This effect is showed up in the experimental observation of low baryon components in the midrapidity region of relativistic heavy-ion collisions at energy of 158A GeV/c (see, e.g. [21]) and in the microscopic model calculations which show the central zone is more baryon dilute than outside zones [22,23]. This effect of "non-homogenous" implies the requirement of a multiple source model to better describe the source of a hadronic gas. The two-source model (TSM) is the simplest multiple source model. In TSM the whole source is roughly divided into two regions (sources): the inner source S_2 and the outer source S_1 . The two sources are supposed to reach equilibrium respectively and possess different temperatures, densities, chemical potentials and other thermodynamic characteristics. Especially the net strangeness density is no longer zero everywhere as in the single-source model but the total number of strangeness still keeps conserved. The two-source model significantly improves the agreement to the experimental data of hadron yields and ratios and exhibits a reasonable source structure [17,18,20]: At SPS and AGS energies, the whole source is composed of a small, hotter core (inner source) surrounded by a large, cooler halo (outer source). Most baryons are distributed outside, seems to be the projectile- and target-like components, while almost all anti-baryons are concentrated inside. Besides, in the two-source model approach, the average particle densities and the average energy density are effectively reduced and the strangeness is effectively suppressed but without introducing extra corrections, such as the corrections of hard core excluded volume of the particles and the strangeness suppression. These corrections were generally used when the whole source is assumed to be a unique homogeneous source.

By means of least square method and by fitting the experimental data, the main thermodynamic characteristics in the two sources, S_2/S_1 , are obtained as follows:

AGS energy the temperatures, T_2/T_1 , are 144/91 MeV. The baryon chemical potentials, μ_{B2}/μ_{B1} , are 288/599 MeV. The strangeness chemical potentials, μ_{S2}/μ_{S1} , are -70.0/116 MeV.

SPS energy $T_2/T_1=168/110$ MeV, $\mu_{B2}/\mu_{B1}=14.4/387$ MeV, $\mu_{S2}/\mu_{S1}=-14.8/52.2$ MeV.

RHIC energy $T_2/T_1=176/175$ MeV, $\mu_{B2}/\mu_{B1}=36.9/38.9$ MeV, $\mu_{S2}/\mu_{S1}=10.0/10.7$ MeV.

The Ω^- yields in above three reactions are directly obtained through formula 2. Because of the large strangeness, -6, and very heavy mass, 3230 MeV, the $(\Omega\Omega)_{0+}$ yields are very small. Therefore, it can be supposed that the thermodynamic quantities would be little effected by the existence of $(\Omega\Omega)_{0+}$. In

Fig. 1. Energy dependence of $(\Omega\Omega)_{0+}$, Ω^- and $(\Omega\Omega)_{0+}/\Omega^-$ in relativistic heavy ion collisions. Points at full RHIC energy, $\sqrt{s_{NN}}=200$ GeV, are obtained by extrapolation. Points at $\sqrt{s_{NN}}=75$ GeV are obtained by interpolation.

statistical model of grand canonical frame, all hadrons in the fireball including $(\Omega^-\Omega^-)_{0+}$ and Ω^- are in chemical and thermal equilibrium. According to formula 2, the yield ratio of $(\Omega\Omega)_{0+}$ to Ω^- has the relation of

$$\eta = \frac{g(\Omega\Omega)}{g\Omega} \left(\frac{m(\Omega\Omega)}{m\Omega} \right)^{3/2} e^{-[(m(\Omega\Omega)-\mu(\Omega\Omega))-(m\Omega-\mu\Omega)]} . \quad (3)$$

With formulas 2 and 3 the $(\Omega\Omega)_{0+}$ yields can be obtained from the Ω^- yields. The yields of $(\Omega\Omega)_{0+}$ and Ω^- together with the ratios are presented in Table 1 (rows 2-4) and shown in Fig. 1.

(put Table 1 here)

Apparently, the yields of $(\Omega\Omega)_{0+}$ and Ω^- increase steadily as the energy increases from AGS to SPS, and to RHIC. At RHIC energy, they are 5.8×10^{-4} and 5.8 respectively. The ratio, however, shows a saturation feature in RHIC energy region with value of $\simeq 1.0 \times 10^{-4}$.

With results in above three reactions, we can try to predict the results for Au+Au collisions at full RHIC energy, $\sqrt{s_{NN}} = 200$ GeV, by means of extrapolation (with Lagrange formula). In order to reduce the effect of system size to the extrapolated results as possible, these three collisions have been chosen to possess the same or similar reaction system. The results are shown in Fig. 1 (last points) and also shown in Table 1 (last column). At RHIC and full RHIC energies, the yields of $(\Omega\Omega)_{0+}$ are 5.8×10^{-4} and 1.2×10^{-3} respectively, well within the limits of the detectors used in RHIC energies. With the excellent characteristics, $(\Omega\Omega)_{0+}$, the marvelous particle, can be easily identified and detected when it is created.

3 Discussion and Summary

In order to justify the reliability of the model predictions, we give out some results related to the strange particles and compare them to the experimental data or other model predictions. Table 2 and Fig.2 show the yields of $\bar{\Omega}^+$, Ω^- and their ratio $\bar{\Omega}^+/\Omega^-$. At low energy the $\bar{\Omega}^+$ yield is much lower than the Ω^- yield, while $\bar{\Omega}^+$ increases faster than Ω^- as the energy increases. So at somewhere they will have equal yield (in the figure, it is at $\sqrt{s_{NN}} \sim 150$ GeV). Table 3 and Fig.3 show the ratios of the anti-strange particle to the strange particle. In Fig.3 the results at AGS energy are for 11.6A GeV/c Au+Au collision used for extrapolations. While in Table 3 the results at AGS energy are for 14.6A GeV/c Si+Au collision used to compare with the available experimental data[9]. For the strange baryons, the ratios possess the similar behavior as the energy increases but the magnitudes are different. Ratio for particle with more strange components is larger than that with less strange components. The ratio of kaon exhibits a different feature which saturates after $\sqrt{s_{NN}} = 70$ GeV with value of 0.8. From the comparisons in Tables 2 and 3, one can see that the model predictions are in very good agreement with the experimental data.

(put Table 2 here)

(put Table 3 here)

Several points need be pointed out. Firstly, the yields and ratios obtained above are thermally produced, i.e. produced in a hot and dense fireball which is assumed to reach the equilibrium or local equilibrium. If taking the kinetic effect into account, some amount of $(\Omega\Omega)_{0+}$ would be produced from two Ω^- 's collision, the total yield of $(\Omega\Omega)_{0+}$ will be a little increased. Secondly, the yields of Ω^- predicted by statistical models generally lower than that given by experiments. So the yields of Ω^- and $(\Omega\Omega)_{0+}$ presented here are the lower limit. Thirdly, more importantly, the experimental data used in calculations for RHIC energy are taken from pseudorapidity interval $|\eta| < 1$ which is a small portion of the whole source of which the rapidity range is $-5.4 < y < 5.4$. (This small portion of source, the "measured" source, is located in the central part of the source. In this region, the particles are uniformly distributed and construct a single homogeneous source. So the two parts, S1 and S2, in TSM are identical (see above the thermodynamic characteristics at RHIC

(put two figures in the same row)

Fig. 2. Energy dependence of $\bar{\Omega}^+$, Ω^- and $\bar{\Omega}^+/\Omega^-$ in relativistic heavy ion collisions. Points at full RHIC energy are obtained by extrapolation. Points at $\sqrt{s_{NN}}=75$ GeV are obtained by interpolation.

Fig. 3. Energy dependence of $\bar{\Lambda}/\Lambda$, $\bar{\Xi}^+/\Xi^-$, $\bar{\Omega}^+/\Omega^-$ and K^-/K^+ in relativistic heavy ion collisions. Points at full RHIC energy are obtained by extrapolation. Points at $\sqrt{s_{NN}}=75$ GeV are obtained by interpolation.

energy) and also identical to the source in the single-source model.) Therefore, if the data are taken from the whole source or a larger rapidity interval, the yields of Ω^- will be raised and correspondingly, the yields of $(\Omega\Omega)_{0+}$ increases. For example, in a conservative estimation, suppose the yield of Ω^- increases two times to reach 12, the yield of $(\Omega\Omega)_{0+}$ increases the same times to reach 1.2×10^{-3} . At full RHIC energy, their yields increase ~ 2.2 times and reach 24 and 2.6×10^{-3} respectively. Obviously, a larger central rapidity range is favorable to measuring the interesting but rarely produced strange dibaryon, $(\Omega\Omega)_{0+}$. Of course, the more exact results are expected after the data of full RHIC energy become available.

So far experimental data are available only for three collisions at AGS, SPS and RHIC energies with the same or similar collision system. There is no data available within the large energy region between SPS and RHIC energies. The particle yields, not as the ratios, are quite sensitive to the "measured" source size or "measured" rapidity interval. Under these limitations, the yields are only roughly estimated and may have large deviation, but it is believable that the order of magnitude would not deviate far away.

In summary, the yields of dibaryon $(\Omega\Omega)_{0+}$, hyperon Ω^- and their ratios in relativistic heavy ion collisions at three energies are calculated within the framework of two-source statistical model. The yields of $(\Omega\Omega)_{0+}$ and Ω^- increase steadily as the energy increases, while their ratios display a saturation feature. By means of extrapolation, the yields and the ratio at full RHIC energy are estimated. In the RHIC energy region, the $(\Omega\Omega)_{0+}$ yield is in order of $10^{-4} - 10^{-3}$, the Ω^- yield is in order of $10^0 - 10^1$ and the ratio of $(\Omega\Omega)_{0+}$ to Ω^- is $\simeq 1.0 \times 10^{-4}$. And, to measure the rarely produced particles as the

strange dibaryon $(\Omega\Omega)_{0+}$, a larger central rapidity range is favorable.

Acknowledgements. The author are grateful to Professors Z.Y. Zhang, Y.W. Yu, C.R. Qing and H.Z. Xo for stimulating discussions. This work is supported by the National Science Foundation of China under the contracts No.19975075.

References

- [1] R.L. Jaffe, Phys. Rev. Lett. **38**, 195 (1977).
- [2] Z.Y. Zhang, Y.W. Yu, P.N. Shen, L.R. Dai, Nucl. Phys. A **625**, 59 (1997).
- [3] P.N. Shen, Y.B. Dong, Y.W. Yu, Z.Y. Zhang and T.S.H. Lee, Phys. Rev. C **55**, 2024 (1997).
- [4] Y.W. Yu, Z.Y. Zhang, X.Q. Yuan, Commun.Theor.Phys. **31**, 1 (1999).
- [5] Z.Y. Zhang, Y.W. Yu, C.R. Ching, T.H. Ho, and Z.D. Lu, Phys. Rev. C **61**, 065204 (2000); Commun.Theor.Phys. **33**, 321 (2000).
- [6] Q.B. Li, P.N. Shen, Z.Y. Zhang, Y.W. Yu, Nucl. Phys. A **683**, 487 (2001).
- [7] E. Anderson, WA97 Collab., Phys. Lett. B **433**, 209 (1998); *ibid.* **449**, 401 (1999).
- [8] S. Margetis, WA49 Collab., J. Phys. G **25**, 189 (1999); F. Gabler, WA49 Collab., J. Phys. G **25**, 199 (1999)
- [9] P. Braun-Munzinger, J. Stachel, J.P. Wessels, and N. Xu, Phys. Lett. B **344**, 43 (1995).
- [10] F. Becattini, J. Cleymans, A. Keranen, E. Suhonen and K. Redlich, Phys. Rev. C **64**, 024901 (2001).
- [11] G.D. Yen and M.I. Gorenstein, Phys. Rev. C **59**, 2788 (1999).
- [12] P. Braun-Munzinger, I. Heppe, J. Stachel, Phys. Lett. B **465**, 15 (1999).
- [13] J. Cleymans and K. Redlich, Phys. Rev. C **60**, 054908 (1999).
- [14] J. Letessier and J. Rafelski, J. Phys. G **25**, 451 (1999); Phys. Rev. C **59**, 947 (1999).
- [15] Z.D. Lu *et al.*, High Energy Phys. Nucl. Phys. **22**, 910 (1998).
- [16] G.D. Yen, M.I. Gorenstein, W. Greiner, S.-N. Yang, Phys. Rev. C **56**, 2210 (1997).
- [17] Z.D. Lu *et al.*, High Energy Phys. Nucl. Phys. **26**, 501 (2002).
- [18] Z.D. Lu, Amand Faessler, C.Fuchs, E.E.Zabrodin, in: Zhuxia Li *et al.*(Eds.),Proc. Conf. on nonequilibrium and nonlinear dynamics in nuclear and other finite system, Beijing, China, 2001, AIP-CP597, pp136-139.
- [19] P. Braun-Munzinger, D. Magestro, K. Redlich, and J. Stachel, hep-ph/0105229.
- [20] Z.D. Lu, Amand Faessler, C.Fuchs, E.E.Zabrodin, nucl-th/0110040.
- [21] G. Ambrosini *et al.*, NA52 Collab., Phys. Lett. B **417**, 201 (1998).

- [22] L.V. Bravina *et al.*, Phys. Rev. C **60**, 024904 (1999); Phys. Rev. C **62**, 064906 (2000).
- [23] J. Sollfrank, U. Heinz, H. Sorge, N. Xu, Phys. Rev. C **59**, 1637 (1999).
- [24] E. Andersen *et al.*, WA97 Collab., J. Phys. G **25**, 171 (1999); Phys. Lett. B **449**, 401 (1999).
- [25] H. Appelshäuese *et al.*, NA49 Collab., Phys. Lett. B **444**, 523 (1998).
- [26] Z. Xu, STAR Collab., nucl-ex/0104001; Nucl. Phys. A **698**, 607 (2002).
- [27] G.S.F. Stephans, E802 Collab., Nucl. Phys. A **566**, 269c (1994).
- [28] T. Abbott *et al.*, E802 Collab., Phys. Rev. C **50**, 1024 (1994).

FIGURE CAPTIONS

Fig 1 Energy dependence of $(\Omega\Omega)_{0+}$, Ω^- and $(\Omega\Omega)_{0+}/\Omega^-$ in relativistic heavy ion collisions. Points at full RHIC energy, $\sqrt{s_{NN}}=200$ GeV, are obtained by extrapolation. Points at $\sqrt{s_{NN}}=75$ GeV are obtained by interpolation.

Fig 2 Energy dependence of $\bar{\Omega}^+$, Ω^- and $\bar{\Omega}^+/\Omega^-$ in relativistic heavy ion collisions. Points at full RHIC energy are obtained by extrapolation. Points at $\sqrt{s_{NN}}=75$ GeV are obtained by interpolation.

Fig 3 Energy dependence of $\bar{\Lambda}/\Lambda$, $\bar{\Xi}^+/\Xi^-$, $\bar{\Omega}^+/\Omega^-$ and K^-/K^+ in relativistic heavy ion collisions. Points at full RHIC energy are obtained by extrapolation. Points at $\sqrt{s_{NN}}=75$ GeV are obtained by interpolation.

Table 1

Yields of $(\Omega^-\Omega^-)_{0+}$ and Ω^- , and their ratios in relativistic heavy ion collisions. Results at full RHIC energy, $\sqrt{s_{NN}}=200$ GeV, are obtained by extrapolation.

	AGS	SPS	RHIC	full RHIC
$(\Omega^-\Omega^-)_{0+}$	9.18×10^{-7}	2.78×10^{-5}	5.78×10^{-4}	1.20×10^{-3}
Ω^-	0.0423	0.444	5.81	10.7
η	2.17×10^{-5}	6.26×10^{-5}	0.996×10^{-4}	1.03×10^{-4}

Table 2

Yields of Ω^- and $\bar{\Omega}^+$, and $\bar{\Omega}^+/\Omega^-$ in relativistic heavy ion collisions. Results at full RHIC energy are obtained by extrapolation.

	AGS	SPS	RHIC	full RHIC
Ω^-	4.23×10^{-2}	0.444	5.81	10.7
$\bar{\Omega}^+$	3.74×10^{-3}	0.166	5.37	12.0
$\bar{\Omega}^+/\Omega^-$	8.84×10^{-2}	0.378	0.926	1.04
		exp: 0.383 ± 0.081 [24,12]	(0.898[19])	(0.941[19])

Table 3

Ratios of anti-strange particle to strange particle in relativistic heavy ion collisions. Results at full RHIC energy are obtained by extrapolation.

	AGS*	SPS	RHIC	full RHIC
$\bar{\Lambda}/\Lambda$	1.40×10^{-3}	0.134	0.738	0.930
	$(2.0\pm 0.8)\times 10^{-3}$ [27,9]	0.131 ± 0.017 [24,12]	0.77 ± 0.07 [26,19]	
$\bar{\Xi}^+/\Xi^-$	1.74×10^{-3}	0.211	0.823	1.00
		0.232 ± 0.033 [25,12]	0.82 ± 0.08 [19]	
$\bar{\Omega}^+/\Omega^-$	8.12×10^{-4}	0.378	0.926	1.04
		0.383 ± 0.081 [24,12]	(0.898[19])	(0.941[19])
K^-/K^+	4.54^{-1}	1.82^{-1}	0.800	0.791
	$(4.4\pm 0.4)^{-1}$ [28,9]	$(1.8\pm 0.1)^{-1}$ [24,12]	$0.88\pm 0.07^{**}$	

* Both data and results are for Si+Au collision at 14.6A GeV/c.

* Average value of four experimental data shown in [19].

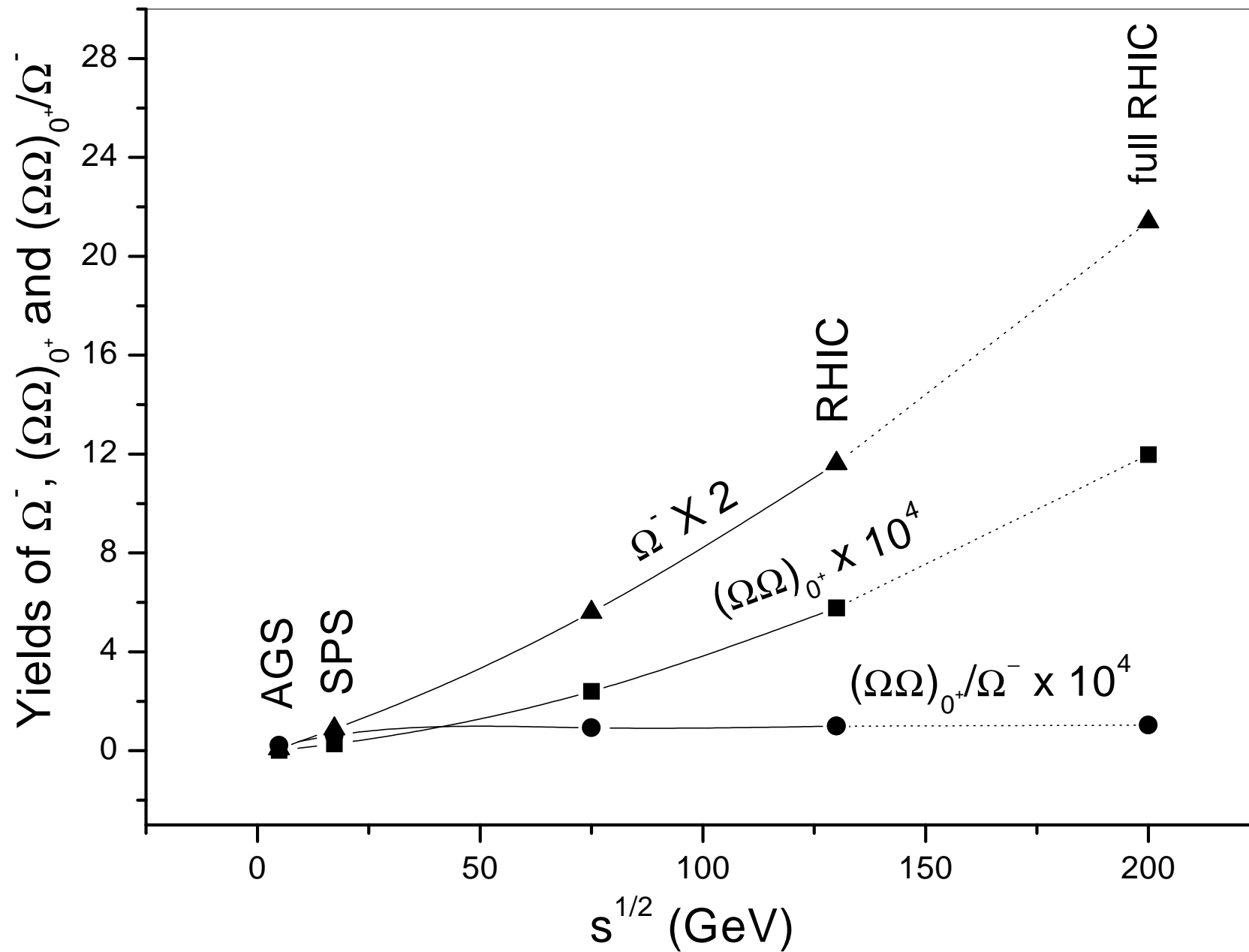


Fig. 1

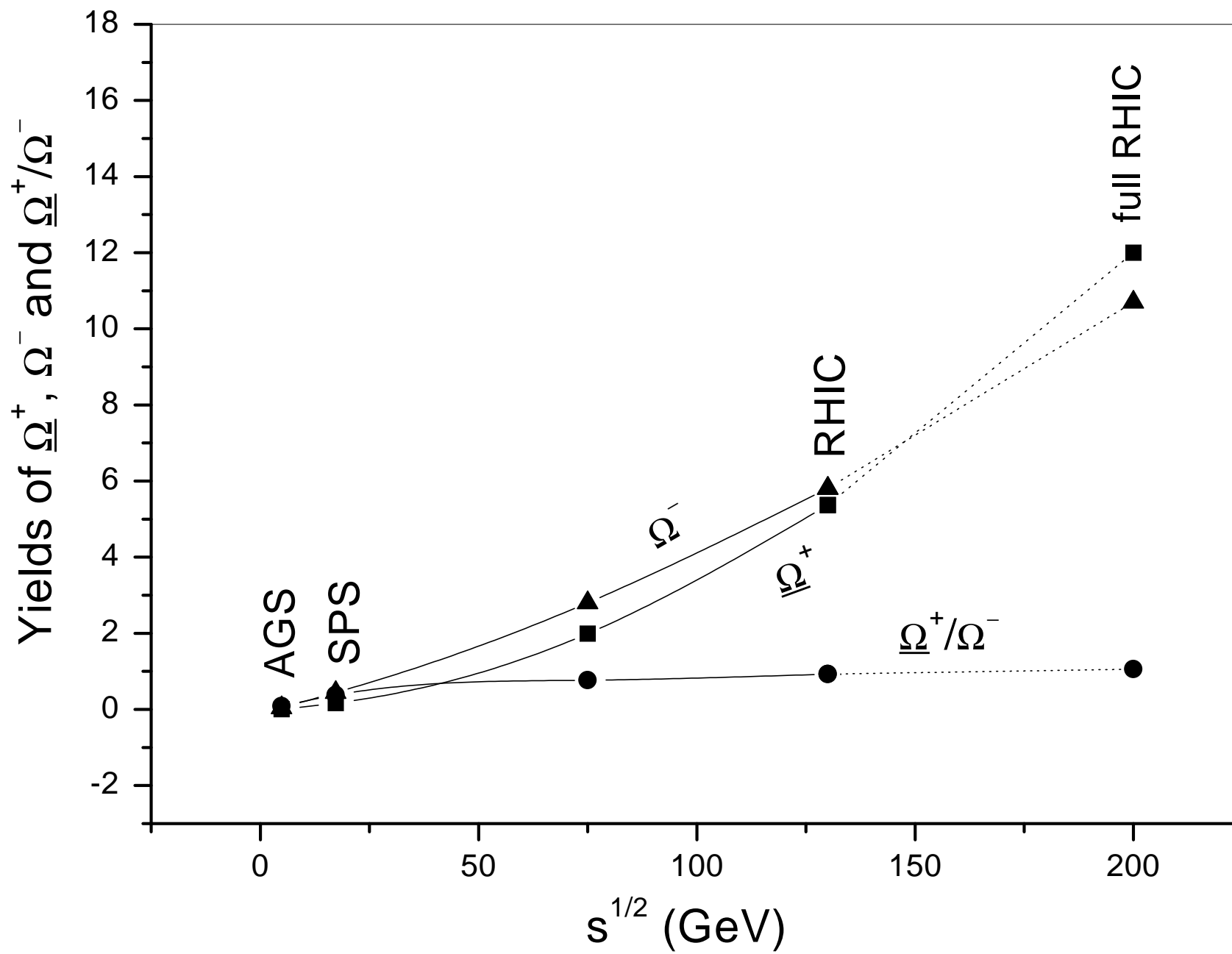


Fig. 2

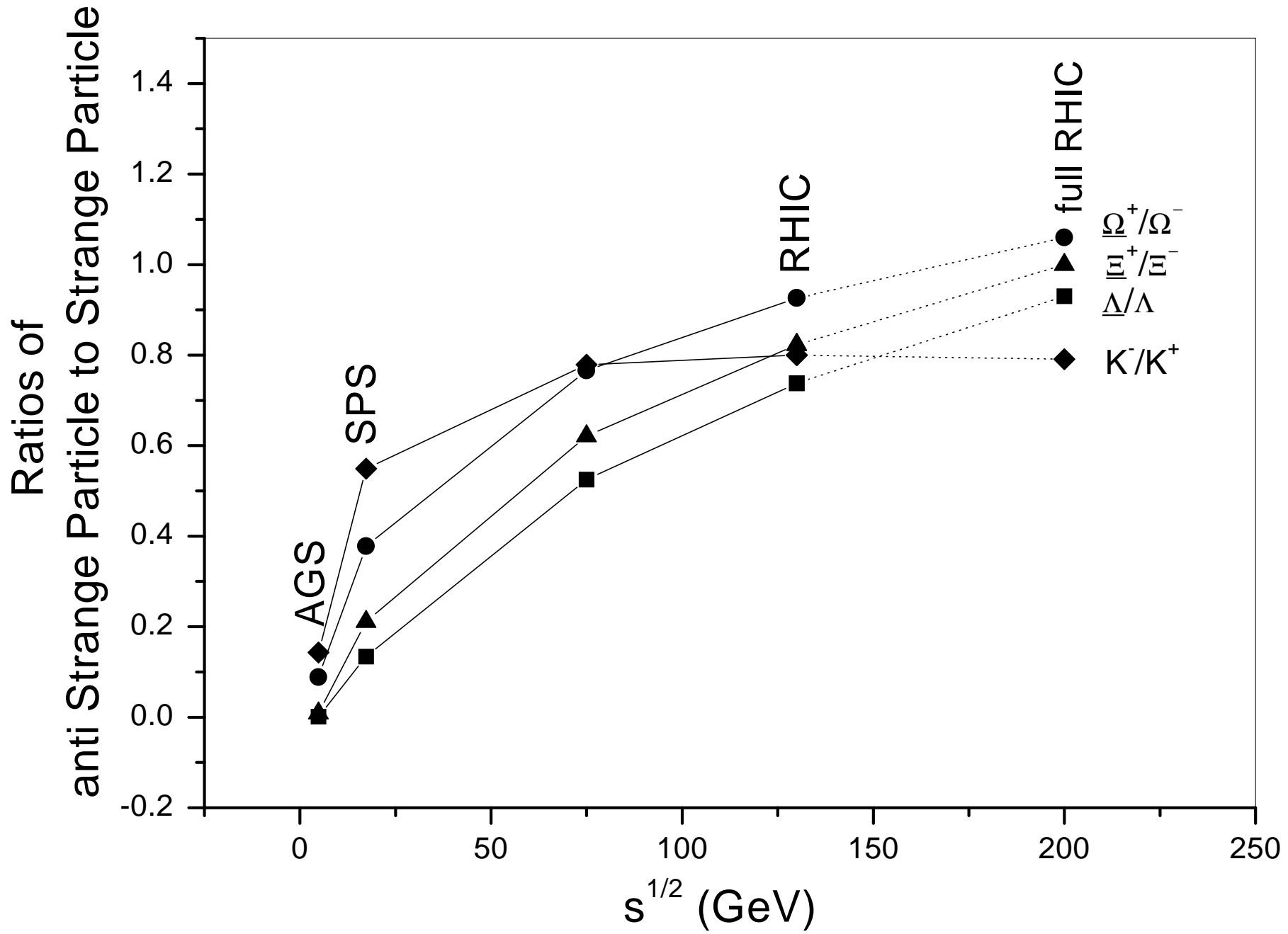


Fig. 3